

# PCCP

Accepted Manuscript



This is an *Accepted Manuscript*, which has been through the Royal Society of Chemistry peer review process and has been accepted for publication.

*Accepted Manuscripts* are published online shortly after acceptance, before technical editing, formatting and proof reading. Using this free service, authors can make their results available to the community, in citable form, before we publish the edited article. We will replace this *Accepted Manuscript* with the edited and formatted *Advance Article* as soon as it is available.

You can find more information about *Accepted Manuscripts* in the [Information for Authors](#).

Please note that technical editing may introduce minor changes to the text and/or graphics, which may alter content. The journal's standard [Terms & Conditions](#) and the [Ethical guidelines](#) still apply. In no event shall the Royal Society of Chemistry be held responsible for any errors or omissions in this *Accepted Manuscript* or any consequences arising from the use of any information it contains.

**The microwave heating mechanism of N-(4-methoxybenzyliden)-4-butylaniline in liquid crystalline and isotropic phases as determined by *in situ* microwave irradiation NMR spectroscopy**

Yugo Tasei<sup>1</sup>, Fumikazu Tanigawa<sup>1</sup>, Izuru Kawamura<sup>1</sup>, Teruaki Fujito<sup>2</sup>, Motoyasu Sato<sup>3</sup>,  
Akira Naito<sup>1,\*</sup>

<sup>1</sup>Graduate School of Engineering, Yokohama National University, 79-5 Tokiwadai, Hodogaya-ku, Yokohama 240-8501, Japan. <sup>2</sup>Probe Laboratory Inc., 1-7-17, Kawasaki, Haruma, Tokyo, 205-0021, Japan. <sup>3</sup>Faculty of Engineering, Chubu University, 200 Matsumoto-cho, Kasugai 457-8501, Japan.

\*Corresponding author. Tel: +81-45-339-4232, Fax: +81-45-339-4251. E-mail address:naito@ynu.ac.jp

Running Title

Microwave heating mechanism of MBBA

## Abstract

Microwave heating effects are widely used in the acceleration of organic, polymerization and enzymatic reactions. These effects are primarily caused by the local heating induced by microwave irradiation. However, the detailed molecular mechanisms associated with microwave heating effects on the chemical reactions are not yet well understood. This study investigated the microwave heating effect of N-(4-methoxybenzylidene)-4-butylaniline (MBBA) in liquid crystalline and isotropic phases using *in situ* microwave irradiation nuclear magnetic resonance (NMR) spectroscopy, by obtaining  $^1\text{H}$  NMR spectra of MBBA under microwave irradiation. When heated simply using the temperature control unit of the NMR instrument, the liquid crystalline MBBA was converted to the isotropic phase exactly at its phase transition temperature ( $T_c$ ) of  $41^\circ\text{C}$ . The application of microwave irradiation at 130 W for 90 sec while maintaining the instrument temperature at  $20^\circ\text{C}$ , generated a small amount of the isotropic phase within the bulk liquid crystal. The sample temperature of the liquid crystalline state obtained during microwave irradiation was estimated to be  $35^\circ\text{C}$  by assessing the linewidths of the  $^1\text{H}$  NMR spectrum. This partial transition to the isotropic phase can be attributed to a non-equilibrium local heating state induced by the microwave irradiation. The application of microwave at 195 W for 5 min to isotropic MBBA while maintaining an instrument temperature of  $50^\circ\text{C}$  raised the sample temperature to  $160^\circ\text{C}$ . In this study, the MBBA temperature during microwave irradiation was estimated by measuring the temperature dependent chemical shifts of individual protons in the sample, and the different protons were found to indicate significantly different temperatures in the molecule. These results suggest that microwave heating polarizes bonds in polar functional groups, and this effect may partly explain the attendant acceleration of organic reactions.

## Introduction

Microwave heating is widely used to accelerate organic reactions,<sup>1-11</sup> to reduce polymerization times,<sup>12-15</sup> and to enhance the activity of enzymes.<sup>16-18</sup> The majority of the reaction acceleration obtained in this manner can be explained by the thermal effect of the microwaves.<sup>19</sup> However, nonthermal effects have also been identified and it has been reported that the thermal and nonthermal effects of microwaves can be separated.<sup>20</sup> The existence of nonthermal effects of microwave has recently been demonstrated by the observation that the rates of polymerization reactions are increased under electric fields but decreased under magnetic fields.<sup>15</sup> The microwave thermal effects are attributed to increases in the solvent temperature due to dielectric loss.<sup>4,5,7,21,22</sup> The solvent molecule dipoles will align with an applied electric field and in the case of microwave irradiation, the applied field will oscillate. As the dipoles attempt to realign with this alternating electric field, heat energy is released by molecular friction and collision. Ions will also translate along the oscillating electric field, generating collisions or friction with other molecules in the sample matrix to produce additional thermal energy. However, the details of the molecular mechanisms associated with the microwave heating effect on chemical reaction rates have not yet been fully elucidated. One of the most important phenomena associated with microwave irradiation is non-equilibrium localized heating, defined as the generation of isolated regions with much higher temperatures than the bulk solution. This has been reported to occur in liquid-solid<sup>23</sup> systems in response to microwave irradiation, such as in the case of dimethyl sulfoxide (DMSO) molecules in contact with Co particles under microwave irradiation.

In the present study, an *in situ* microwave irradiation solid state NMR spectrometer was developed with the aim of characterizing microwave heating mechanisms. The

technique of microwave irradiation liquid state NMR spectrometer was first envisioned by Naito et al.<sup>24,25</sup> and was used to obtain state-correlated two-dimensional (2D) NMR spectra. This allowed high resolution observation of  $^1\text{H}$  dipolar patterns in  $^1\text{H}$  NMR spectra in the liquid state rather than the liquid crystalline state. Using this method, the local dipolar interactions of individual protons in the liquid crystalline state can be examined via high resolution resonance in the isotropic phase<sup>26-28</sup> and the resulting data may also be used to obtain state-correlated two dimensional NMR spectra of proteins in both native and denatured states.<sup>29</sup> During microwave irradiation process, electron dipole moments are excited, leading to heating of the sample. This differ from excitation of electron spin magnetic moments, as occurs in electron spin resonance (ESR) and dynamic nuclear polarization (DNP) experiments.

Liquid crystalline samples are known to absorb microwaves with high efficiency, since they necessarily contain polar functional groups. It is therefore expected that microwave heating phenomena will be more readily observed in liquid crystals. Thus, an *in situ* microwave irradiation solid state NMR spectrometer set-up was designed specifically to obtain NMR signals during microwave irradiation. This system isolated the effects of the radio waves applied to obtain the NMR detection from the microwaves employed to generate local heating. This spectroscopic technique thus allowed clear NMR signals to be obtained while simultaneously applying microwave irradiation.

In the present study, microwave heating effects were characterized using a sample of the liquid crystal N-(4-methoxybenzylidene)-4-butylaniline (MBBA). This compound was chosen, since liquid crystalline samples exhibit both highly efficient microwave heating and high boiling points. It was necessary to accurately measure the temperature of the sample during microwave irradiation and in this work, the variation in the  $^1\text{H}$

chemical shifts were employed as an indicator of temperature. In the case of diamagnetic nuclei, it has been reported that the temperature dependence of chemical shift values are typically linear in nature,<sup>30-34</sup> and we therefore assessed the temperature of the MBBA sample based on the temperature dependent-chemical shifts of the protons in the MBBA molecule.

### Materials and Methods

A sample of N-(4-methoxybenzyliden)-4-butylaniline (MBBA) was purchased from the Tokyo Chemical Industry Co., Ltd. and used without further purification. The liquid crystal to isotropic phase transition temperature ( $T_c$ ) of this compound is reported to occur at 41 °C.<sup>35</sup>

The temperature of a sample within an NMR spectrometer is normally regulated by the set point of the temperature control unit integrated into the instrument. In the present work, however, it was important to directly measure the temperature of the sample itself, since microwave heating was expected to increase the sample temperature and cause this temperature to depart from the setting of the instrument. It can be physically challenging to accurately measure the actual temperature of an NMR samples under microwave irradiation due to the wide special variations in temperature throughout the bulk of the sample. For these reasons, the temperature-dependent chemical shift values of the sample were instead used as a temperature indicator. The difference in the chemical shifts,  $\Delta\delta$ , of the  $\text{CH}_3$  and OH protons of methanol or glycol are commonly used for the purposes of temperature calibration in NMR spectrometers.<sup>30,31</sup> In the case of methanol, the relation between  $\Delta\delta$  and temperature is not completely linear over a wide temperature range, and so a quadratic relationship is instead applied, with an associated error of 0.6

K. Over narrow temperature range, however, the plot of  $\Delta\delta$  as a function of temperature can be fit by a straight line with a minimal associated temperature error. In the case of glycol, the data can be perfectly fit by a straight line over a wide temperature range.<sup>30</sup> The  $^{31}\text{P}$  chemical shift dependence of a paramagnetic lanthanide complex with temperature has also been shown to generate a straight line over a narrow temperature range,<sup>32</sup> although the chemical shift dependence of nuclei with paramagnetic electrons typically exhibit an inverse relationship with temperature. Variation of the chemical shifts of water protons in a bicelle sample vs. temperatures shows linear in the temperature range of 10 to  $-60\text{ }^\circ\text{C}$ .<sup>33</sup> In solid state NMR studies, the variation in  $^{207}\text{Pb}$  chemical shifts with temperature have exhibited linear relationship over the temperature range of  $-130$  to  $+150\text{ }^\circ\text{C}$ .<sup>34</sup> Based on these previous reports, the variation in the  $^1\text{H}$  chemical shift values of individual protons of the MBBA sample were assessed with regard to their variation with temperature. The resulting plots of chemical shifts as functions of temperature obtained from microwave irradiation were subsequently evaluated by assuming that the relationships between these chemical shifts and temperature were approximately linear.

The instrument used in this work consisted of a Chemagnetics solid state NMR spectrometer (CMX infinity 400) equipped with a microwave generator (IDX, Tokyo Electronics Co., Ltd.) capable of transmitting 1.3 kW pulsed or continuous microwave at a frequency of 2.45 GHz. This apparatus allowed us to obtain NMR signals without interference while simultaneously applying microwave irradiation. A 3 mm wide flat copper ribbon was used to form the capacitor of the resonance circuit, and was wound coaxially inside the radio wave circuit to reduce arcing and to increase isolation during microwave irradiation (see Figure S1). The microwave resonance circuit was tuned to 2.45 GHz and the radio wave was set to 398 MHz using a sweep generator. Microwaves

were transmitted from the microwave generator to the vicinity of the magnet through the waveguide, which served a coaxial cable and finally the microwaves were guided to the resonance circuit at the probe head. The microwave pulses were controlled by the gating pulses produced by the pulse programmer of the NMR spectrometer. The sample was initially cooled to obtain the liquid crystalline phase using the temperature control unit of the spectrometer. Samples were packed in an inner glass tube to insulate them from thermal contact with the outer glass tube.

## Results

### *Microwave heating of liquid crystalline MBBA*

Figure 1A gives the molecular structure of MBBA. Figure 1B shows the  $^1\text{H}$  NMR spectra of MBBA in the liquid crystalline state at  $35\text{ }^\circ\text{C}$ , which is  $6\text{ }^\circ\text{C}$  below its phase transition temperature ( $T_c$ ) of  $41\text{ }^\circ\text{C}$ . A broad  $^1\text{H}$  NMR spectrum with a 20 kHz linewidth was obtained in the liquid crystalline sample due to  $^1\text{H}$ - $^1\text{H}$  dipolar couplings. Since MBBA molecules are aligned to the magnetic field in the liquid crystalline phase, residual  $^1\text{H}$ - $^1\text{H}$  dipolar interactions cause a number of transitions with various dipolar interactions and this generates the observed line broadening. These dipolar interactions can provide information concerning the order parameters of liquid crystals. A high resolution  $^1\text{H}$  NMR spectrum of MBBA in the isotropic phase was also obtained at  $45\text{ }^\circ\text{C}$ , in which numerous proton signals were resolved and assigned to the various protons in the molecule,<sup>36</sup> as shown in Figure 1C.

In subsequent trials, the MBBA temperature was increased from  $20.0\text{ }^\circ\text{C}$ , which is  $20.5\text{ }^\circ\text{C}$  below  $T_c$ , to  $40.5\text{ }^\circ\text{C}$  which was experimentally determined  $T_c$  using the spectrometer's temperature control unit. As shown in Figure 2A,  $^1\text{H}$  NMR signal of the



liquid crystalline phase appeared alone at 35 °C. At 40.0 °C, liquid crystalline phase had partly transitioned to the isotropic phase (Figures S2). It was observed that the temperature of liquid crystal and isotropic phases were nearly same. It was also evident that the signals obtained at this temperature were broader than those of the fully isotropic phase, which may be attributed to the interaction of the isotropic and liquid crystalline phases. This phase transition was completed at 40.5 °C (Figure 2B, Figure S2-F), which indicates that liquid crystal and isotropic phases coexisted near the phase transition temperature.

The instrument temperature was then set at 20 °C, (20.5 °C below  $T_c$ ), followed by continuous wave (CW) microwave irradiation. The application of 130 W for 90 sec generated weak isotropic phase signals (representing approximately 2% of bulk sample) among the liquid crystalline phase signals (Figures 2C and also see Figure S3-A). Based on the temperature dependence of the linewidths, the temperature of the liquid crystalline phase was estimated to 35 °C by assessing the linewidths of the NMR signals (Figure 3). Normally, such signals would not be expected until the temperature of the sample is close to its isotropic phase transition temperature of 40.5 °C as seen in setting by temperature control unit. The linewidth of the isotropic phase generate under these conditions was slightly narrower than that of the isotropic phase obtained by heating at 40.0 °C via the temperature control unit (Figure 2C and Figure S2-E). This result indicates that microwave irradiation generated localized heating in the sample to form regions of the higher temperature isotropic phase.

Typically, the temperature of locally heated regions obtained from microwave irradiation has been difficult to detect experimentally. Using *in situ* microwave irradiation NMR, however, the temperature of the sample was successfully determined, since the

temperature of the liquid crystal MBBA was correlated with the NMR linewidths, as shown in Figure 3. As noted, microwaves irradiation generated a small fraction of the isotropic phase in the bulk liquid crystal at 35 °C, even though this is 5.5 °C lower than the phase transition temperature of the 40.5 °C, suggesting a non-equilibrium localized heating within the sample.

#### *Microwave heating of isotropic MBBA*

In these trials, the instrument temperature was set at 50 °C and various power settings (65, 130 and 195 W) were used to irradiate the MBBA in the isotropic phase. As shown in Figure 4, the individual proton signals were shifted to higher fields with the application of greater amount of power for 10 min and different protons exhibited different degrees of chemical shifts. It is also evident that the linewidths were broadened by irradiation with higher power, although the chemical shift dependence on temperature is typically very small in diamagnetic compounds. These results indicate that the temperature of the MBBA sample was increased significantly and that the spatial temperature distribution was also very pronounced during microwave irradiation.

It is well known that the chemical shift values of a sample are affected by its temperature.<sup>30-34</sup> In the case of diamagnetic nuclei, the variation in chemical shift values with temperature are approximately linear. Therefore, the chemical shift values of individual protons were determined as functions of temperature for MBBA in the isotropic phase, as shown in Figure 5. The chemical shift values did not vary greatly with temperature, when the temperature was increased by 30 °C, for example, a higher field shift of only 0.06 ppm was observed for the aromatic protons. Interestingly, the chemical shifts of different protons also had very different the temperature variation. However, the

chemical shift did exhibit a linear change as a function of temperature for each different proton and thus it was possible to estimate the effective temperature of MBBA in the isotropic phase as induced by the microwave irradiation.

Figure 6 presents the MBBA sample temperature increase in response to CW microwave irradiation. Applying 65 W of CW microwave irradiation, increased the temperature from 50 to 70 °C within 2 min based on the majority of protons data, after which the temperature plateaued. However, there were significant variations in the apparent temperatures; the 7' and  $\alpha'$  protons indicated 110 and 80 °C, respectively. When 130 W was applied, the temperature was increased to 140 °C according to the majority of the protons data, although values of 210 and 330 °C were indicated by the  $\alpha'$  and 7' protons, respectively, and 8 min was required to obtain a stable temperature. The temperature of 7' and  $\alpha'$  protons more significantly deviated from the others. Temperature increased by 15 °C during microwave irradiation at 130 W for 90 sec in the liquid crystalline phase (Figure 3). On the other hand, temperature increased by 20 °C during microwave irradiation at 65 W for 1 min (Figure 7) in the isotropic phase. Thus, temperature increase of isotropic phase was larger than that of liquid crystalline phase, and hence, isotropic phase more efficiently absorbs microwave than the liquid crystalline phase. Applying 195 W increased the temperature to 160 °C within 5 min, although again the  $\alpha'$  and 7' protons were discrepant, indicating 220 and 350 °C, respectively. Thus, at this microwave power level, large temperature variations were evident among protons in the same molecule, indicating that individual protons within the same molecule experienced different temperatures.

As noted, it is difficult to determine the temperature of samples during microwave irradiation, because the bulk temperature measured using a thermometer is not always an

accurate representation due to significant variation in temperature throughout the sample. This work found that the analysis of chemical shifts can determine the temperatures of individual moieties within the sample molecules.

Figure 7A makes it evident that the  $\gamma'$  and  $\alpha'$  protons evidently experienced much higher temperature than those of other protons in the same molecule. As shown in Figure 7B, however, the temperature indicated by protons other than  $\gamma'$  and  $\alpha'$  were all very similar and hence they are considered to represent the temperature of the bulk isotropic state. Thus, the temperature at a power of 65 W could be determined accurately, since the chemical shift values were within the range of experimentally determined values using temperature controlled unit of instrument.

## Discussion

### *Mechanism of microwave heating effects on liquid crystalline MBBA*

The microwave-induced local heating phenomena observed in the liquid crystalline MBBA can be explained as shown schematically in Figures 8A, B, C and D. Here, heating the liquid crystalline phase, initially below its phase transition temperature, by microwave irradiation (indicated by “MW”) to a temperature near the  $T_c$ , generates a small amount of the isotropic phase inside the sample (Figure 8B). Because the dielectric loss of the isotropic phase is expected to be higher than that of the liquid crystalline phase, the isotropic phase is heated more efficiently by microwave irradiation, inducing a relatively high temperature in the isotropic phase region. This phenomenon can be considered as a kind of non-equilibrium localized heating state. These isotropic phases form small particles and the surfaces of these particles interact with the surrounding liquid crystal to generate different linewidths compared to those produced by the bulk isotropic phase. As

this isotropic phase loses thermal energy to the liquid crystalline phase, the sharp signals of the isotropic phase transition back to the broad signals of the liquid crystalline phase. This allows us to distinguish the microwave-induced isotropic phase from the liquid crystalline phase. This non-equilibrium heating state can be maintained over long time spans because the rate at which heat is obtained by the small isotropic phase particles by absorbing microwave energy balanced the rate at which heat is dissipated to the bulk liquid crystalline phase. At higher power levels, the bulk isotropic phase appears (Figure 8C) and, eventually, the entire sample transitions to the isotropic phase (Figure 8D). Conversely, increasing the temperature solely by thermal heating (TH) without microwave irradiation (Figures 8E, F and G), causes the isotropic phase to appear at the surface of the sample (Figure 8F). There, when a temperature nearly equal to the phase transition temperature is applied, an equilibrium state is achieved in which the temperature of the isotropic phase is the same as that of the liquid crystalline phase.

Similar non-equilibrium local heating phenomena under microwave irradiation have been reported for liquid-solid<sup>23</sup> mixtures. In the present study, the microwave irradiation of MBBA generated a non-equilibrium localized heating state that could be maintained for long time spans, in which an isotropic phase was present within the neat liquid crystalline state, solely as the result of the microwave irradiation.

#### *Mechanism of microwave heating effects on isotropic phase MBBA*

It is of interest to consider the reason why the  $\gamma'$  and  $\alpha'$  protons of the MBBA molecules showed significantly different chemical shifts from the other protons. Since the chemical shifts had a linear relation with temperature, the  $\gamma'$  and  $\alpha'$  protons also indicated significantly higher temperatures than the other protons, suggesting that these individual

protons might actually have experienced different temperatures.

It is not, however, ruled out the possibility that the slopes of the chemical shifts of these two protons as a function of temperature deviate from linearity at high temperatures, thus generating exceptionally large chemical shifts in the higher temperature range.

However, another theory may be advanced by considering that both protons are associated with the polar bonds of the H-C=N- and CH<sub>3</sub>-O- functional groups. Irradiation of the MBBA sample produces strong electric field that may interact with these polar groups to generate dielectric polarization which reduce the entropy term of the system. This reduction of entropy term gives additional energy to the system which has been gained thermal energy arising from the molecular friction to rise the temperature. Consequently, the electron density experienced by the  $\gamma'$  and  $\alpha'$  protons increase slightly, producing higher field chemical shift changes during microwave irradiation. It should be pointed out that microwave energy at 2.45 GHz is far from affecting any change in the electron density through excitation of electronic state. This energy of the entropy term causes deviation from the linear temperature increase by thermal energy. This energy increase of the polar group may in turn affect the rates of various chemical reactions. This kind of temperature increase of the particular protons bonded to polar group may discuss as a distinctive microwave effect as mentioned as thermal and non-thermal microwave effects.<sup>5,37</sup>

It is important to note that this study has shown that microwaves can increase the temperatures of samples with large dipole moments in a short span of time and can achieve significantly elevated temperatures during the measurement of NMR signals. Therefore, microwaves have potential as a heating source in NMR spectrometers. This effect could also be used for rapid temperature rise experiments such as have been

performed using a liquid crystalline isotropic phase with correlated 2D NMR spectroscopy.<sup>24-28</sup>

The *in situ* microwave irradiation NMR spectroscopy makes it possible to observe organic reaction<sup>1-7</sup> and protein denaturation<sup>29</sup> pathways under microwave irradiation together with the structural information. These observations provide the information on the thermal and non-thermal microwave effects on the organic reaction in the atomic resolution, although it is controversial to distinguish them.<sup>5,37</sup> Furthermore, applications of the microwave rapid temperature jump experiments enabled to perform a state correlated 2D NMR spectroscopy which provides <sup>1</sup>H-<sup>1</sup>H dipolar interaction with the resolution of isotropic phase<sup>24-28</sup> and hence allow to apply the technique to more complicated liquid crystalline samples as demonstrated using advanced 2D separated local field NMR.<sup>38,39</sup>

## Conclusion

An *in situ* microwave irradiation NMR spectrometry technique was developed in which spectra were acquired simultaneously with microwave heating of liquid crystalline samples of MBBA. Analysis of the temperature dependence of the linewidths demonstrated that non-equilibrium localized heating of the sample generated regions of the isotropic state in which the temperature was higher than that of the bulk liquid crystal. These non-equilibrium localized zones may cause significant acceleration of chemical reactions. It was also shown that significantly elevated temperatures can be rapidly achieved using *in situ* microwave irradiation in conjunction with NMR spectroscopy. Finally, the temperatures indicated by the  $\gamma'$  and  $\alpha'$  protons of the MBBA molecules were significantly higher than those of the other protons. These protons are bonded to polar

functional groups, and hence it is possible that microwave irradiation induced increased electron polarization in the associated bonds. This polarization would result in changes in the chemical shifts and may partly explain the mechanism by which organic reactions are accelerated through the distinctive microwave effects.

### **Acknowledgment**

This work was supported by Grants-in-Aid for Scientific Research on a Priority Area (24121709) and an Innovative Area (26102514 and 26104513), and a Grant-in-aid for Scientific Research (C) (24570127) from the Ministry of Education, Culture, Sports, Science and Technology of Japan.



## Notes and references

† Electron Supplementary Information (ESI) available: [Figures S1, S2 and S3].

1. R. Gedye, F. Smith, K. Westaway, H. All, L. Baldisers, L. Laberge and J. Rousell, *Tetrahedron Lett.*, 1986, **27**, 279-282.
2. R. J. Giguere, T. L. Bray, S. M. Duncan and G. Majetcih, *Tetrahedron Lett.*, 1986, **27**, 4945-4948.
3. D. Adam, *Nature*, 2003, **421**, 571-572.
4. L. Perreux and A. Loupy, *Tetrahedron* 2001, **57**, 9199-9223.
5. P. Lidström, J. Tiemey, B. Nathey and J. Westman, *Tetrahedron*, 2001, **57**, 9235-9283.
6. D. Bogdal, M. Lukasiewicz, J. Pielichowski, A. Miciak and Sz. Bednarz, *Tetrahedron*, 2003, **59**, 649-653.
7. C. O. Kappe, *Angew. Chem. Int. Ed.*, 2004, **43**, 6250-6284.
8. Y. Yoshimura, H. Shimizu, H. Hinou and S. -I. Nishimura, *Tetrahedron Lett.*, 2005, **46**, 4701-4705.
9. M. C. Parker, T. Besson, S. Lamare and M. D. Legoy, *Tetrahedron Lett.*, 1996, **46**, 8383-8386.
10. H. Shimizu, Y. Yoshimura, H. Hinou and S. -I. Hishimura, *Tetrahedron*, 2008, **64**, 10091-10096.
11. C. O. Kappe, B. Pieber and D. Dallinger, *Angew. Chem. Int. Ed.*, 2013, **52**, 1088-1094.
12. R. Hoogenboom, F. Wiesbroch, H. Huang, M. A. M. Leenen, H. M. L. Thijs, S. F. G. M. van Nispen, M. van der Loop, C. -A. Fustin, A. M. Jonas, J. -F. Goby and U.S. Schubert, *Macromolecules*, 2006, **39**, 4719-4725.
13. T. Iwamura, K. Ashizawa and M. Sakaguchi, *Macromolecules*, 2009, **42**, 5001-5006.
14. Y. Kajiwara, A. Nagai and Y. Chujo, *Polymer J.*, 2009, **41**, 1080-1084.

15. S. Yamada, A. Takasu, S. Takayama and K. Kawamura, *Polym. Chem.*, 2014, **5**, 5283-5288.
16. B. N. Pramanik, U. A. Mirza, Y. H. Ing, Y. -H. Liu, P. L. Bartner, P. C. Weber and A.K. Bose, *Protein Science*, 2002, **11**, 2676-2687.
17. W. Huang, Y. -M. Xia, H. Gao, Y. -J. Fang, Y. Wang and Y. Fang, *J. Mol. Catalysis*, 2005, **35**, 115-116.
18. S. -S. Lin, C. -H. Wu, M. -C. Sun and Y.-P. Ho, *J. Am. Soc. Mass Spectrom.*, 2005, **16**, 581-588.
19. M. A. Herrero, J. M. Kremsner and C. O. Kappe, *J. Org. Chem.*, 2008, **73**, 36-49.
20. D. Obermayer, B. Gutmann and O. Kappe, *Angew. Chem. Int. Ed.*, 2009, **48**, 8321-8324.
21. M. Tanaka and M. Sato, *J. Chem. Phys.*, 2007, **126**, 034509.
22. M. Kanno, K. Nakamura, E. Kanai, K. Hoki, H. Kono, M. Tanaka, *J. Phys. Chem. A*, 2012, **116**, 2177-2183.
23. Y. Tsukahara, A. Higashi, T. Yamauchi, T. Nakamura, M. Yasuda, A. Baba and Y. Wada, *J. Phys. Chem. C*, 2010, **114**, 8965-8970.
24. A. Naito, M. Imanari and K. Akasaka, *J. Magn. Reson.*, 1991, **92**, 85-93.
25. A. Naito and M. Ramamoorthy, Structural Studies of Liquid Crystalline Materials Using a Solid State NMR Technique. Thermotropic Liquid Crystal: Recent Advances. Springer, 2007, p85-116.
26. A. Naito, M. Imanari and K. Akasaka, *J. Chem. Phys.*, 1996, **105**, 4502-4510.
27. K. Akasaka, M. Kimura, A. Naito, H. Kawahara and M. Imanari, *J. Phys. Chem.*, 1995, **99**, 9523-9529.
28. A. Naito and Y. Tasei, *Materials Science and Technology (MS&T)*, 2010, 2886-2894.

29. K. Akasaka, A. Naito and M. Imanari, *J. Am. Chem. Soc.*, 1991, **113**, 4688-4680.
30. A. L. Van Geet, *Anal. Chem.*, 1968, **40**, 2227-2229.
31. A. L. Van Geet, *Anal. Chem.* 1970, **42**, 679-680
32. C. S. Zuo, K. R. Metz, Y. Sun and A. D. Sherry, *J. Magn. Reson.*, 1998, **133**, 53-60.
33. S. V. Dvinskikh, K. Yamamoto, U. H. N. Dürr and A. Ramamoorthy, *J. Magn. Reson.* 2007, **184**, 228-235.
34. A. Bielecki and D. P. Burum, *J. Magn. Reson., Ser. A*, 1995, **116**, 215-220.
35. H. Kelker and B. Scheurle, *Angew. Chem. Int. Ed.*, 1969, **8**, 884-885.
36. J. S. Prasad, *J. Chem. Phys.*, 1976, **65**, 941-944.
37. A. de la Hoz, Á. Diaz-Ortiz and A. Moreno, *Chem. Soc. Rev.*, 2005, **34**, 164-178.
38. T. Narasimhaswamy, D. -K. Lee, K. Yamamoto, N. Somanathan and A. Ramamoorthy, *J. Am. Chem. Soc.*, 2005, **127**, 6958-6959.
39. K. Nishimura and A. Naito, *Chem. Phys. Lett.*, 2006, **419**, 120-124.

Figure captions

Fig. 1. (A) Molecular structure of N-(4-methoxybenzyliden)-4-butylaniline (MBBA).  $^1\text{H}$  NMR spectra of MBBA at (B) 35 °C in the liquid crystalline phase and (C) 45 °C in the isotropic phase, together with signal assignments of the individual protons.<sup>35</sup>

Fig. 2.  $^1\text{H}$  NMR spectra (left) and expanded spectra (right) of MBBA at (A) 35 and (B) 40.5 °C and setting the temperature at 20 °C under 130 W CW microwave irradiation for (C) 90 and (D) 140 sec.

Fig. 3. Plot of the line widths of  $^1\text{H}$  NMR spectra of MBBA at various temperature as regulated by the instrument temperature control unit (blue square). The red square indicates the temperature (35 °C) of MBBA in the liquid crystalline state following microwave irradiation at 130 W for 90 sec, in which a small amount of the isotropic phase appeared within the liquid crystalline bulk.

Fig. 4.  $^1\text{H}$  NMR spectra (left) and expanded spectra (middle and right) of MBBA in the isotropic phase at (A) 50 °C and under CW microwave irradiation of (B) 65, (C) 130 and (D) 196 W for 10 min while regulating the instrument temperature at 50 °C.

Fig. 5. Plots of  $^1\text{H}$  chemical shift values of MBBA for individual protons against temperatures regulated by the instrument's temperature control system.

Fig. 6. Plots of temperatures against microwave irradiation time at microwave powers of

(A) 65, (B) 130 and (C) 195 W. Temperatures were determined using the slopes obtained for the individual protons.

Fig. 7. Plots of temperatures against microwave irradiation times under microwave irradiation at 65 W for (A) the  $\gamma'$  and  $\alpha'$  protons (blue symbols) and (B) the remainder of the protons. The black line in both plots indicates the average temperature of the remainder of the protons.

Fig. 8. Schematic diagrams showing the proposed (A, B, C and D) microwave (MW) and (E, F and G) thermal heating (TH) processes within the liquid crystalline state. During microwave irradiation, a small fraction of the liquid crystalline domain changes to the isotropic phase (image B). The rate of temperature increase in this isotropic phase domain is higher than in the liquid crystalline phase because the dielectric loss of the isotropic phase is larger than in liquid crystalline phase. This may be considered to represent a non-equilibrium localized heating state. In contrast, thermal heating transition a small fraction of the liquid crystalline state to the isotropic phase at the surface of the sample (image F). When applying thermal heating using the instrument's temperature control unit, the temperature of the isotropic phase is the same as that of liquid crystalline state.

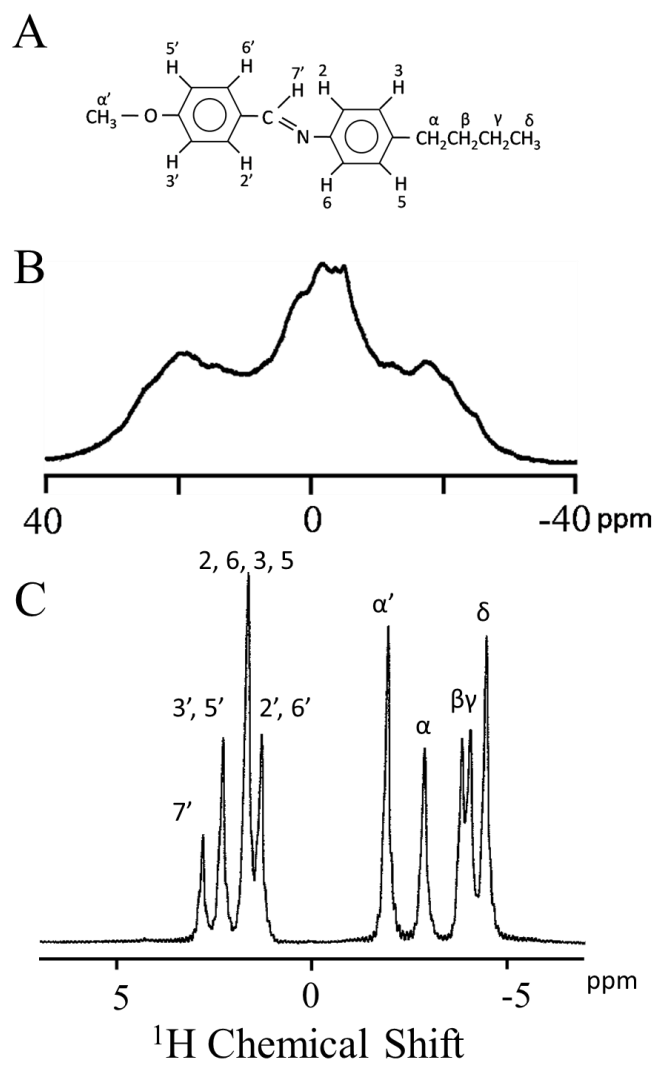


Fig. 1 Tasei et al.

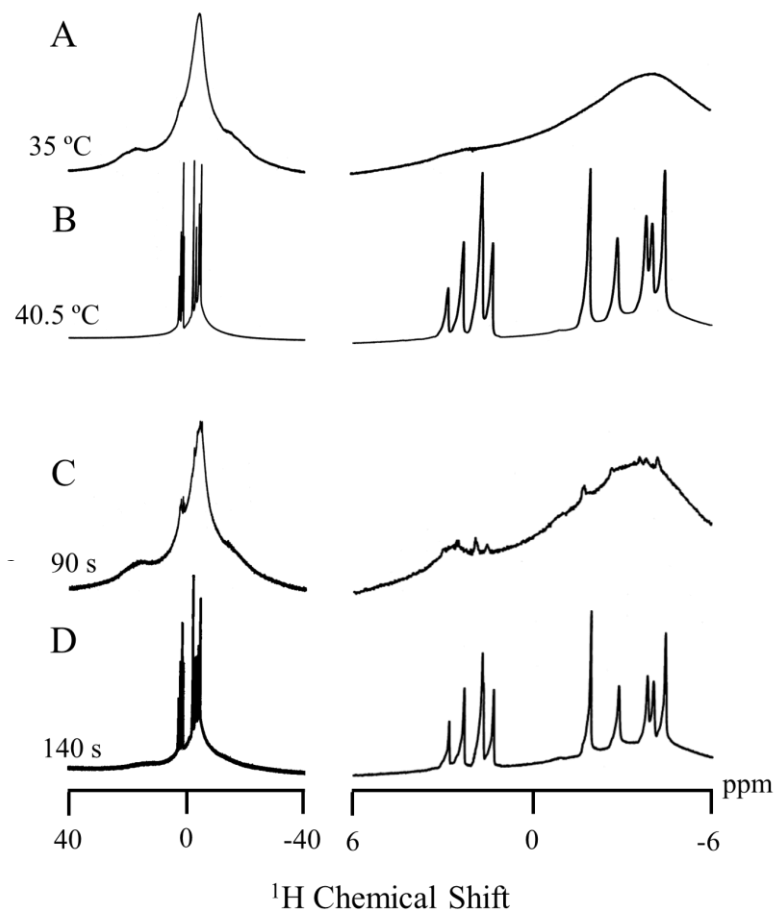


Fig. 2 Tasei et al.

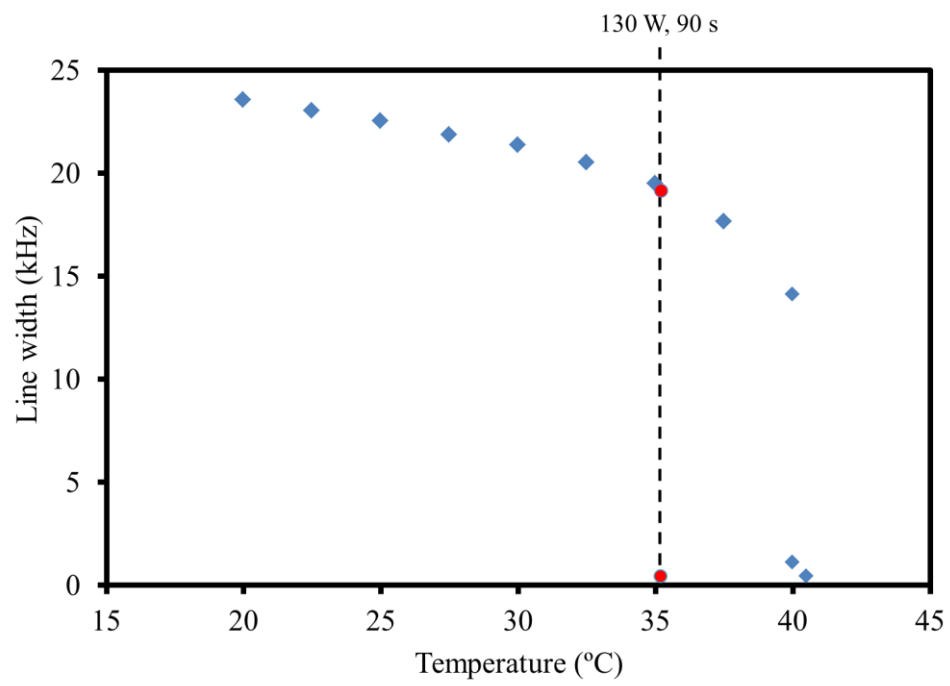


Fig. 3 Tasei et al.



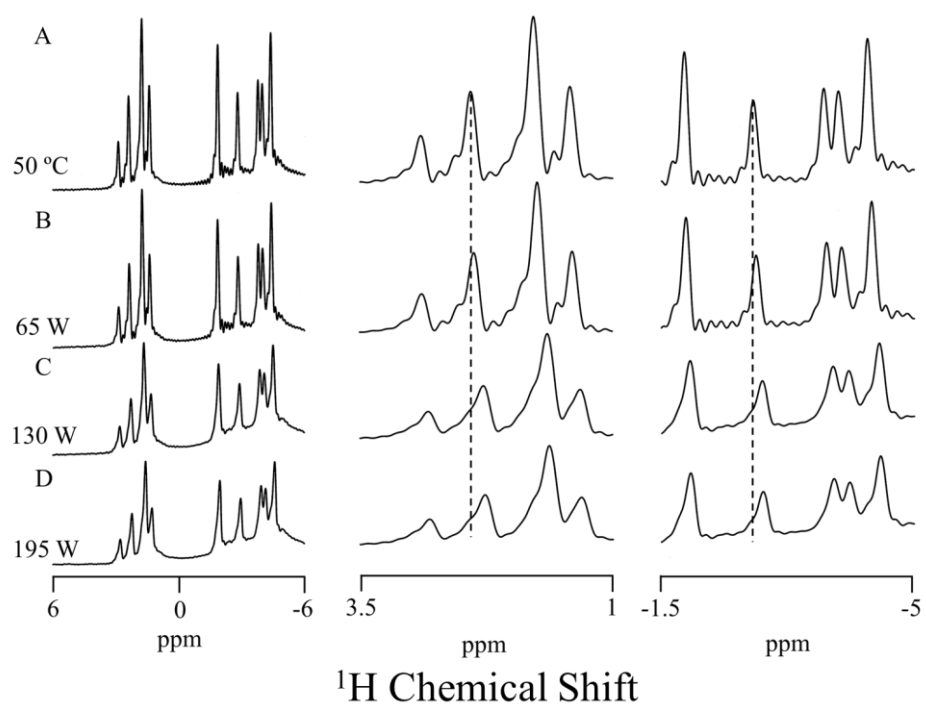


Fig. 4. Tasei et al.

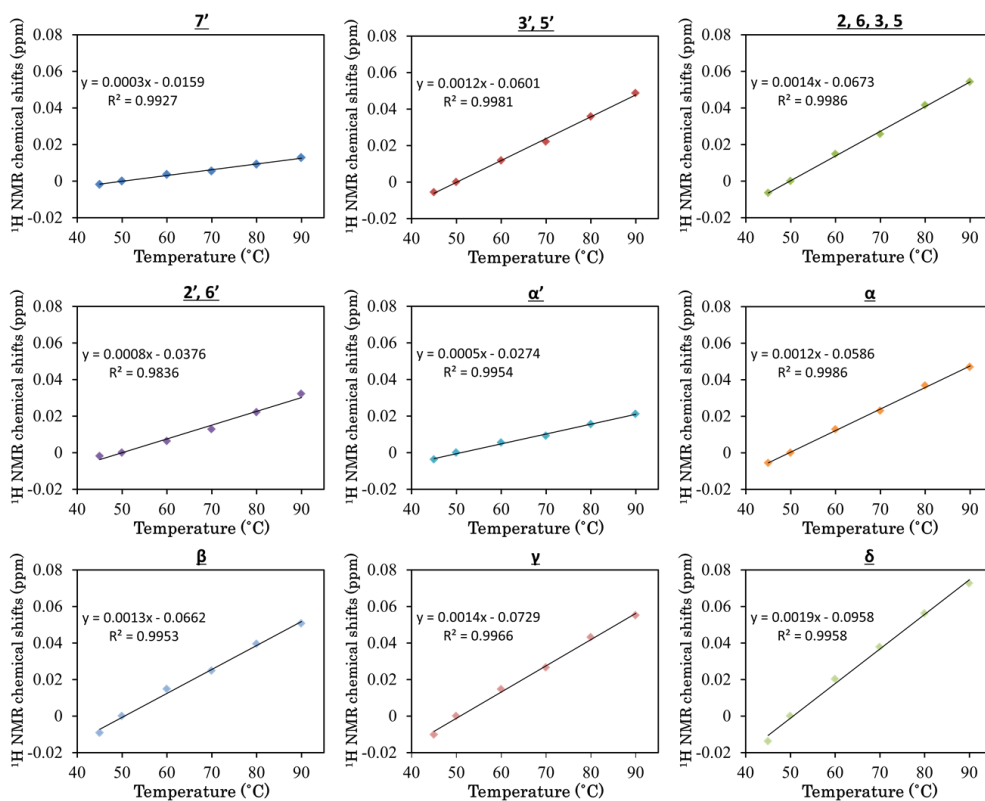


Fig. 5. Tasei et al.

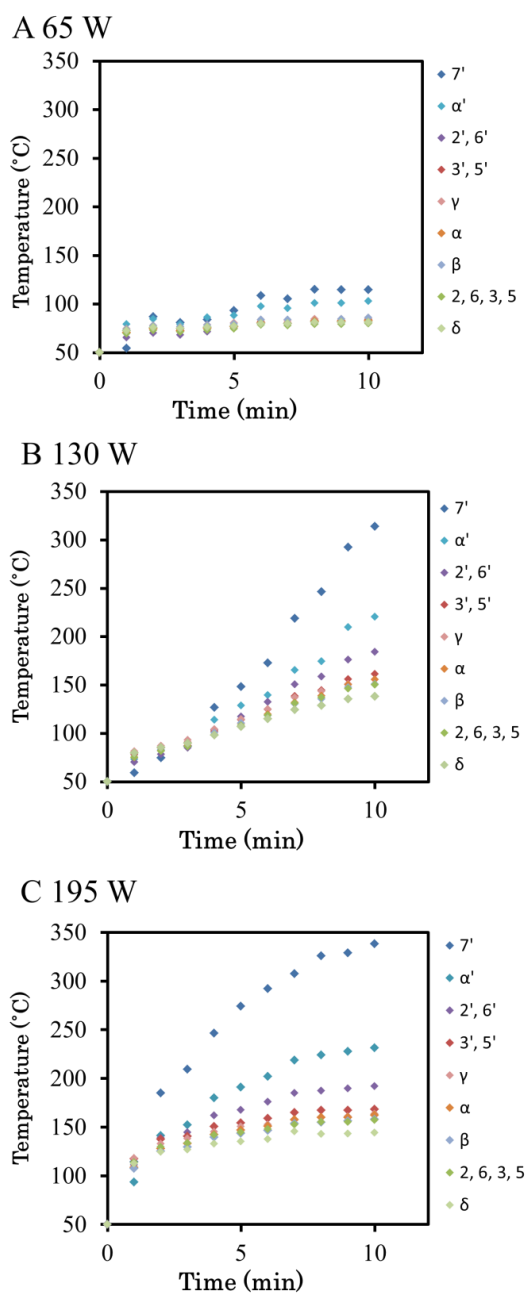


Fig. 6. Tasei et al.

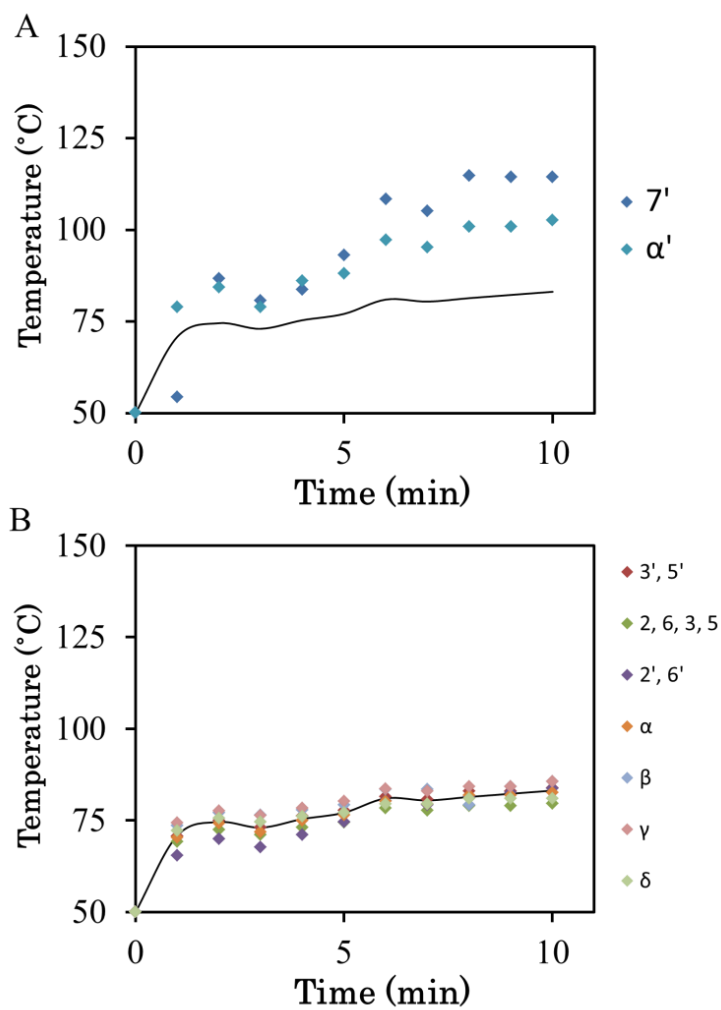


Fig. 7. Tasei et al.

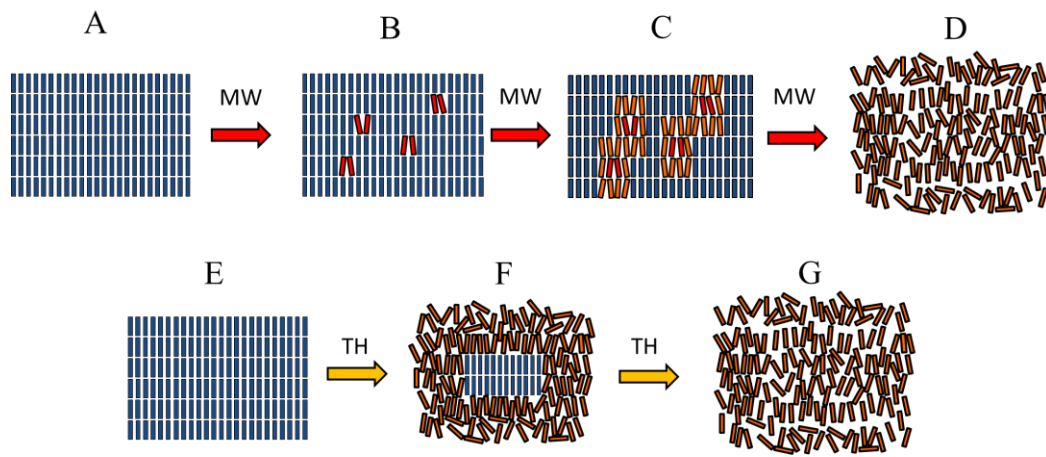


Fig. 8. Tasei et al.